

Journal Pre-proof

Alternative methods for calculating compaction in sedimentary basins

Manuel Martín-Martín, Pedro Robles-Marín

PII: S0264-8172(19)30584-7

DOI: <https://doi.org/10.1016/j.marpetgeo.2019.104132>

Reference: JMPG 104132

To appear in: *Marine and Petroleum Geology*

Received Date: 2 June 2019

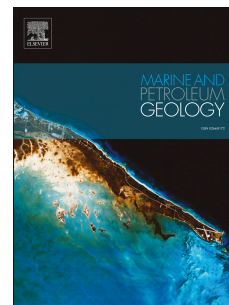
Revised Date: 6 September 2019

Accepted Date: 8 November 2019

Please cite this article as: Martín-Martín, M., Robles-Marín, P., Alternative methods for calculating compaction in sedimentary basins, *Marine and Petroleum Geology* (2019), doi: <https://doi.org/10.1016/j.marpetgeo.2019.104132>.

This is a PDF file of an article that has undergone enhancements after acceptance, such as the addition of a cover page and metadata, and formatting for readability, but it is not yet the definitive version of record. This version will undergo additional copyediting, typesetting and review before it is published in its final form, but we are providing this version to give early visibility of the article. Please note that, during the production process, errors may be discovered which could affect the content, and all legal disclaimers that apply to the journal pertain.

© 2019 Published by Elsevier Ltd.



Clean copy

Marine and petroleum geology

Alternative methods for calculating compaction in sedimentary basins

Manuel Martín-Martín¹ and Pedro Robles-Marín²

¹Departamento de Ciencias de la Tierra y Medio Ambiente, University of Alicante, AP-99, E-03080, Alicante, Spain

²Departamento de Ingeniería Civil, University of Alicante, AP-99, E-03080, Spain

Corresponding author: Manuel Martín-Martín (orcid.org/0000-0002-5797-9892), manuel.martin.m3@gmail.com.

Abstract

Subsidence analysis is an important technique in the study of sedimentary basins but the effects of compaction must be “backstripped”. The compaction of sediments is also of importance for petroleum and water reservoir research with very important economic derivations. Most methods for calculating compaction are based on empirically derived porosity-depth relationships from a variety of known sediment types. The challenge of this paper is to apply alternative methods for calculating compaction in sedimentary basins based on: physical calculation with elastic by Steinbrenner, oedometric and change of the specific weight of the sediment methods; and use of Loadcap software. The Triassic to Lower Miocene 3025 m thick succession of Sierra Espuña (SE Spain) is used as case study for the calculations. In this

28 succession former mineralogical studies and apatite fission-track suggested an original thickness
29 between 4 and 6 km. The validity of each one of the proposed methods is discussed, as well as,
30 compared for the whole succession compaction but also separately for hard vs soft sediments
31 and for thick vs thin beds. The compaction values obtained with the alternative methods are
32 similar to those resulting with the lower-limit curves of the porosity-depth change method. The
33 new methods have provided values slightly higher than 4 km for the whole original thickness
34 using the geotechnical software and the change of the sediments specific weigh methods;
35 meanwhile values below 4 km for other methods. So, in our opinion, the geotechnical software
36 and the change of the specific weight of the sediment methods are compatible with
37 mineralogical constraints and also, the input data are usually better known and easier to
38 determinate. Otherwise, the elastic method seems only accurate for soft sediments; meanwhile
39 the oedometric method is highly influenced by the thickness of the considered beds.

40

41 **Keywords:** Sediments compaction calculating, physical calculation, use of geotechnics-
42 engeneering software, basin analysis, Sierra Espuña succession.

43

44 **1. Introduction**

45 Subsidence analysis is central to the study of sedimentary basins (Allen and Allen, 1990; *and*
46 *refereces therein*). Several types of stratigraphic data are needed to perform this kind of
47 analysis, such as a detailed stratigraphic column showing present-day thicknesses, types of
48 lithologies, ages of horizons, and estimated paleodepths (Watts and Ryan, 1975; Van Hinte,
49 1978; Watts, 1978; Watts, 1981).

50 There are three main elements to consider in the subsidence analysis procedure (Van Hinte,
51 1978; Mayer, 1987): sedimentary record of the basin, compaction and paleobathymetry. The
52 present day thickness and the exact lithology of each stratigraphic unit of a basin must be
53 collected. At effect of compaction must be removed in order to estimate the original thickness of
54 sediments. As sedimentary units compact after deposition, the thicknesses measured today are

55 smaller than those deposited. The changes (if those took place) in paleowater depth must also be
56 taken into account to avoid underestimating the true amount of basin subsidence and also
57 because that water loading can also result in compaction.

58 The effects of sediment compaction must be “backstripped” and most of the methods used for
59 calculating compaction are based on empirically derived porosity-depth relationships from a
60 variety of sediment types (Steckler and Watts, 1978; Bond *et al.*, 1983; Kominz *et al.*, 2011).
61 Those methods seek to calculate the thickness of a sedimentary unit at the time of deposition
62 according to the decrease in porosity of the sediment during burial. In these calculations it is
63 assumed that volume of grains does not change during the burial, no significant diagenesis takes
64 place, and porosity decreases with depth. Troubles arise with the effects of overpressured
65 horizons, the cementation and diagenesis, and with the exact lithologies involved (Allen and
66 Allen, 1990). Recent studies indicate that the change of porosity with depth is exponential until
67 a certain depth, meanwhile at deeper depths the curves show uniform porosity (compaction
68 proceeds extremely slowly) due to the decrease in hydroconductivity at higher pressures
69 (Fowler and Yang, 1998; 1999). Two types of mechanical compaction therefore have to be
70 considered: poroelastic at shallow depth (the most important) while viscoelastic at great depth
71 (with less importance) (Yang, 2001; Cheauveau and Kaminski, 2008). For other authors
72 (Stefaniuk and Mackowski, 2000) the former types take place in two phases: a syngenetic (early
73 and of the utmost importance) and a postgenetic (later and almost negligible). A large number of
74 compaction curves for several lithologies appear in literature with great differences among them
75 (Marcusen, 2009) and, in some cases, for the compaction of a concrete lithology, a range of
76 variability (with low- and upper-limits) is proposed (Bond *et al.*, 1983). Moreover, stratigraphic
77 units usually are made of a mixture of lithologies (Kominz *et al.*, 2011). Also, the role of the
78 mineral content of sediments seems to influence the capability of compaction of sediments
79 (Marcusen *et al.*, 2009; Bjorlykke, 2014).

80 Some published works explored other ways for determining compaction (Meckel *et al.*, 2006;
81 2007; Cheauveau and Kaminski, 2008). Therefore, numerical models using elastoplastic
82 mechanical and chemical concepts (Schneider *et al.*, 1996), or geotechnical data of modern

83 depositional environments (Meckel *et al.*, 2006; 2007), have been introduced. In some cases,
84 compaction is lower than expected (Meckel *et al.*, 2006; 2007). Other numerical calculations are
85 based on the Burger-type model to determine the implications of transient rheology for viscous
86 compaction (Cheauveau and Kaminski, 2008), or in other cases, as in Mars, the lack of empiric
87 studies has propelled researchers to explore other numerical calculations (Gabasova and Kite,
88 2018).

89 This is a challenge of main important because the role of compaction is not only central in
90 determining the subsidence of sedimentary basins, but also for migration of petroleum and
91 water reservoirs, which have very important economic derivations (Fowler and Yang, 1998;
92 Suetnova and Vasseur, 2000; Cheauveau and Kaminski, 2008; Marcusen *et al.*, 2009; Benjamin
93 and Nwachukwu, 2011; Bjorlykke, 2014; *among others*).

94 Taking into account the aforementioned, this paper applies other known methods for calculating
95 compaction in sedimentary basins. The proposed alternative methods for compaction modeling
96 are of two types: (1) physical calculation by elastic method (Steinbrenner, 1936), oedometric,
97 and change of the specific weight of the sediments; (2) use of geotechnical and engineering
98 software for calculating compaction. The validity of each one of the proposed methods is
99 discussed, as well as, compared with the results obtained using two curves of change of porosity
100 with depth from literature.

101 The input values used for the calculations are measured in field, are standards derived from
102 literature tables and/or supplied by a company of geotechnical studies - Esfera Consultores. This
103 company has conducted laboratory tests on unconsolidated sediments from the floors of the
104 harbors and of consolidated sediments at a certain depth of these same harbors. In any case, the
105 same values of final thicknesses, physical properties, coefficients and modules are used in the
106 different methods allowing a valid comparison.

107 The Mesozic-Cenozoic succession of Sierra Espuña (SE Spain), with a outcropping Mesozoic
108 and Cenozoic complete marine succession (Martín-Martín *et al.*, 1997; Martín-Martín *et al.*,
109 2006a,b; Perri *et al.*, 2017), is used as the case study for the calculations.

110

111 2. Methods

112 The application of alternative methods for calculating compaction tries to reproduce the
113 conditions in sedimentary basins from the beginning of sedimentation (when soft sediments are
114 deposited on marine or lacustrine floors) to the exhumation of the basin, while passing through
115 the burial to depths of about 4000 m for the older beds. There are three phases of sediment
116 evolution in sedimentary basins during burial (Allen and Allen, 1990): (1) unconsolidated
117 sediments; (2) consolidated sediments; and much later, (3) lithified sediments (sedimentary
118 rocks), when diagenesis processes, cementation and main compaction took place as well. Main
119 compaction happens in early phases when sediments are soft and saturated with water (Fowler
120 and Yang, 1998; 1999; Stefaniuk and Mackowski, 2000; Yang, 2001; Cheauveau and Kaminski,
121 2008). In these early phases, pores are reduced and water is expelled during the burial due to the
122 loading of successive beds. Total compaction is the sum of the compactions in the three stages.
123 Young and Oedometric Modules and Poison Coefficient are used in appropriate way for the
124 aforementioned stages of sediments. These are standards derived from literature tables for
125 lithified sediments; and supplied by a company of geotechnical studies - Esfera Consultores.
126 This company has conducted laboratory tests on unconsolidated sediments from the floors of the
127 harbors and of consolidated sediments at a certain depth of these same. Usually, the Young and
128 Oedometric Modules for lithified sediments are of an order of magnitude 100 times greater than
129 those of unconsolidated sediments. Therefore, the obtained compactions for lithified sediments
130 are of less than 5 % than those of unconsolidated sediments, compaction in this phase being
131 almost negligible when compared with the compaction suffered before the lithification.

132 This section introduces the methods from literature and other alternative methods proposed in
133 this paper, for calculating compaction. The section is divided into the following sub-sections:
134 (2.1) the backstripping procedure (necessary for obtaining the original thickness in a
135 sedimentary basin analysis; (2.2) the traditional method for calculating compaction with
136 porosity-deph change empiric curves; (2.3) methods of physical calculation applied to calculate
137 compaction; (2.4) the elastic by Steinbrenner method; (2.5) the oedometric method; (2.6)

138 Change of specific weight of the sediment; (2.7) Methods based on the use of geotechnical
139 software (the loadcap engineering software). Although most of these methods (elastic,
140 oedometric, loadcap software) are developed for a rectangular load on a rigid base and
141 calculated as a shortening due to compaction in the surface of the load, the compaction can be
142 calculated for fractions of 1/3 of the width of a rectangle and 10,000 m have been estimated for
143 that width.

144

145 *2.1. The backstripping procedure*

146 In the application of the proposed methods for calculating compaction, a backstripping
147 procedure must be performed to obtain the original thickness of the stratigraphic levels.
148 Backstripping uses the standard technique (Steckler and Watts, 1978; Sclater and Christie, 1980;
149 Allen and Allen, 1990; Roberts *et al.*, 1998; Wagneich and Schmid, 2002; Van Sickle *et al.*,
150 2004; *among others*) by isolating the stratigraphic units one-by-one, and then sequentially
151 removing or backstripping in reverse order. By successive backstripping, the deepening history
152 of the basin can be plotted in several steps, one for each “stripped off” stratigraphic units. In the
153 case of the Sierra Espuña Succession, 18 stratigraphic levels are considered (Table 1), so 17
154 backstripping steps have been performed in each method.

155

156 *2.2. Porosity-depth change (traditional method)*

157 This method seeks to estimate the thickness of a sedimentary unit at the time of deposition (T_0)
158 according to the decrease in porosity of sediment during burial. This is the traditional method
159 used in literature in determining the compaction. In these calculations it is assumed that the
160 volume of grains does not change during the burial and porosity decreases exponentially with
161 depth. Several empirical curves are proposed in literature (Steckler and Watts, 1978; Sclater and
162 Christie, 1980; Bond *et al.*, 1983; Poelchau *et al.*, 1997; Marcussen, 2009; *among others*). We
163 have obtained the original and final porosity from the curves from Steckler and Watts (1978)
164 and from Bond *et al.* (1983). The first one is a single smoothed exponential curve valid for all

165 lithologies. In all cases of this curve, the original porosity of the rocks is close to 55 %,
 166 meanwhile the end porosity depends on the burial. The second (Bond *et al.*, 1983), is a set of
 167 double exponential lithology-dependent curves with a low- and upper limits of compaction of
 168 the same lithology. In addition, in the case of the lower-limit an early cementation is assumed
 169 for carbonate and siliceous rocks. In this second curve the original porosity can range from 20 to
 170 80% depending on the original lithology, meanwhile the present porosity also depends on the
 171 depth, but according to the lithological types. In both cases, the original thickness is obtained
 172 from Equation 1 from Van Hinte (1978), where ϕ_0 is the original porosity, T_N is the thickness
 173 measured today and ϕ_N the present-day porosity. ϕ_0 and ϕ_N can be corrected for large
 174 thicknesses of the stratigraphic units (Bond and Kominz, 1984).

$$175 \quad T_0 = T_N \frac{(1 - \phi_N)}{(1 - \phi_0)} \quad (1)$$

176

177 *2.3. Methods based on physical calculation*

178 Three proposed methods for physical calculation are: elastic (Steinbrenner, 1936), oedometric,
 179 and change of specific weight of the sediment. The input values used for these calculations
 180 are the final thicknesses of the stratigraphic units (measured in the field), the specific weight
 181 (initial and final), the oedometric and elastic modules and the Poisson coefficient. The physical
 182 properties are standards obtained from tables from literature and also from real data coming
 183 from engineering and geotechnical studies by the Company Esfera Consultores de
 184 Construcción. In any case, in all the methods the same values have been used allowing a valid
 185 comparison.

186

187 *2.4. Elastic by Steinbrenner*

188 This method (Steinbrenner, 1936) was derived for a rectangular load on a rigid base and
 189 calculated as the shortening due to compaction in the surface of the load (s_c) through the
 190 Equation 2 (Schleicher, 1926) and the shortening (s_z) in depth (z) of the compressed bed (with
 191 an indefinite thickness) through the Equation 3. The compaction can be calculated for fractions

192 of 1/3 of the width of a rectangle (10,000 m have been estimated for that width). The total
 193 shortening is the difference between the two former values. The estimated initial thickness of
 194 the beds has been considered to be the depth (z) in all the cases. This value must be
 195 backstripped each time a new layer (with its respective load) is superimposed.

$$196 \quad s_c = 2kqb \frac{(1-\nu^2)}{E'} \quad (2)$$

$$197 \quad s_z = \frac{qb}{2E'} (A\phi_1 - B\phi_2) \quad (3)$$

198

199 In these equations k is a shape coefficient depending on a and b , q is the increase of effective stress
 200 in the top of the compressible bed (depending of the specific weight), a is the length and b is the
 201 width in shape of the load bed, z is the initial thickness of the compressible bed, ν is the Poisson
 202 coefficient, E' is the elastic module of the compressible bed, A is equal to $1 - \nu^2$, B is $1 - \nu - 2\nu^2$,
 203 and ϕ_1 and ϕ_2 (Steinbrenner, 1936) are parameters depending on a , b and z . This method considers
 204 compressible materials in a consolidated-sediment state and does not take into account the
 205 previously suffered shortening (in an unconsolidated-sediment state). For this unconsolidated
 206 shortening, a reduction, according to literature (Feiner et al. 1976; Ministerio de Fomento, 2009)
 207 has been previously introduced to the materials: 3% for mostly granular materials, 4 % for mostly
 208 carbonated, 5% for mostly clayey. Calculation for the lithified phase has also been performed with
 209 the same procedure as for unconsolidated sediments but using appropriate elastic modules. Total
 210 compaction is obtained as the sum of the compactions in the three stages (unconsolidated
 211 sediments, consolidated sediments and lithified sediments).

212

213 2.5. Oedometric

214 This method (Terzaghi and Peck, 1976; Barnes, 2000; Atkinson, 2007) allows the estimation of
 215 the shortening considering oedometric conditions of load, i.e., the effective stress increase is
 216 constant throughout the compressible bed. This method has some constraints: (1) the main
 217 compaction is produced in the unconsolidated stage and due to the thickness and weigh of the

218 bed itself; (2) each bed is homogeneous and saturated in water; (3) the permeability coefficient
 219 and the oedometric Module are constants and Darcy Law is fulfilled; (4) the compaction is
 220 mainly due to pore reduction. This method has been applied assuming an initial unconsolidated
 221 stage for the sediments of compressible beds, later, a stage of consolidated sediments, and
 222 finally a stage of lithified sediments. Total compaction obtained is the sum of the compactions
 223 in the three stages. The oedometric module for the unconsolidated stage is lithological
 224 dependent and has been obtained from literature and also from real data coming from
 225 engineering and geotechnical studies from the Company Esfera Consultores de Construcción.
 226 Otherwise, for the consolidated one, the value has been obtained from Equation 4, of common
 227 application in geotechnical studies (Jiménez Salas *et al.*, 1980; Rodríguez Ortíz, *et al.*, 1995), E_m
 228 being the oedometric module, E' the elastic module and ν' the Poisson coefficient.

$$229 \quad E_m = E' \frac{1 - \nu'}{1 - \nu' - 2\nu'^2} \quad (4)$$

230 In both phases the shortening is obtained through the normal equation of the oedometric method
 231 (Equation 5).

$$232 \quad \Delta H = H_0 \Delta \sigma' \frac{1}{E_m} \quad (5)$$

233 In this case, ΔH is the shortening of the compressed bed, H_0 the initial thickness of the former, $\Delta \sigma'$
 234 the increase of effective stress in the middle point (of the initial thickness) of the compressed bed
 235 (depending on the specific weight) and E_m its oedometric module. $\Delta \sigma'$ for initial unconsolidated
 236 stage has been determined as a fraction (2/3) of load of the bed itself; meanwhile in the
 237 consolidated stage corresponds with the load of the overlaying one. Calculation for the lithified
 238 phase has also been performed with the same procedure as for consolidated sediments only now
 239 using the appropriate oedometric modules.

240

241 2.6. Change of specific weight of the sediment

242 This method considers conditions without important changes in the weight of sediments.
 243 Therefore it can be calculated what are the initial conditions using the Equation 6 and the final

244 conditions using Equation 7, γ being the specific weight, W the weight, V the volume, H the
 245 thickness and S the surface of each bed, meanwhile the subscripts $_o$ and $_f$ belong to the initial
 246 and final stages respectively.

$$247 \quad \gamma_o = \frac{W}{V_o} = \frac{W}{H_o S} \quad (6)$$

$$248 \quad \gamma_f = \frac{W}{V_f} = \frac{W}{H_f S} \quad (7)$$

249 Operating in both former equations to isolate W/S and making this relation equal in both
 250 equations, Equation 8 can be obtained, which provides the initial thickness according to the final
 251 thickness and the initial and final specific weights of each bed.

$$252 \quad \gamma_o H_o = \gamma_f H_f \implies H_o = H_f \frac{\gamma_f}{\gamma_o} \quad (8)$$

253 This method is based on similar principles to that of the porosity method, but the specific weight is
 254 a parameter which is much less variable than the porosity, and is much easier and quicker to obtain
 255 through laboratory analysis. Nevertheless, in this work these values have been obtained from the
 256 large amount of related literature (Rodríguez Ortiz *et al.*, 1995; Grundbau-Taschenbuch, 1980;
 257 NAVFAC DM 7-1 y 7-2, 1986; González de Vallejo, 2002) and also from real data coming
 258 from engineering and geotechnical studies from the Company Esfera Consultores de
 259 Construcción.

260

261 *2.7. Methods based on the use of geotechnical software*

262 The program “Loadcap” by “Geostru Software” licensed to the University of Alicante
 263 (reference nº G38RJ2), traditionally used in geotechnical studies to calculate the compaction of
 264 sediments with an embankment overload, is used in this study for calculating compaction
 265 suffered by sediments. To calculate the compaction, the program requires the thickness, the
 266 mean saturated density and the mean oedometric module (a parameter related to the stretching
 267 and the % of pores in the sediments or rocks, and by extension, to the capability of compaction)
 268 of each stratigraphic unit of the basin. The saturated density and the oedometric module are

269 standards and are easily obtained from literature tables (Jiménez-Salas, 1975; González de
270 Vallejo, 2002). The mean density used is saturated since sediments take place in water realm.
271 For the stratigraphic units the mean oedometric modules were calculated in three conditions:
272 when the unit is the last deposited (unconsolidated sediments), when a new bed is deposited and
273 the former sediments have been compacted (consolidated sediments), and when two or more
274 beds have been deposited and sediments have been lithified (sedimentary rocks). The mean
275 density and the mean oedometric module were calculated according to the aforementioned
276 stages in each case and the thickness of each bed composing the sedimentary record. The
277 possibility of overconsolidated beds can also be considered as an input in the program.

278

279 **3. Geological framework of the proposed case study succession**

280 The Sierra Espuña area is located in the west of Murcia province in SE Spain (Fig. 1A)
281 belonging to the Betic Cordillera from the Western Alpine Perimediterranean Orogen (Guerrera
282 *et al.*, 1993). This area (Fig. 1B) is structured as an antiformal stack (Martín-Martín and Martín-
283 Algarra, 2002; Martín-Martín *et al.*, 2006b). In the antiformal stack of Sierra Espuña six
284 tectonic units crop out. The detachment level of the thrusts of the entire area is the Paleozoic-
285 Triassic boundary, being the Paleozoic almost entirely removed by tectonic lamination (Martín-
286 Martín and Martín-Algarra, 2002). The upper two units (Morrón de Totana and Perona,
287 respectively) include a Triassic to Tertiary sedimentary cover. The Morrón de Totana unit
288 shows one of the most developed, thick and well preserved Meso-Cenozoic succession of the
289 central-western Mediterranean area (Martín-Martín *et al.*, 2006a, b; Critelli *et al.*, 2008; Critelli,
290 2018; Perri *et al.*, 2013, 2017) and is of great interest for our purposes being almost completely
291 composed of a Triassic to Early Miocene succession (Tables 1 to 6). The thicker sections of this
292 succession have been selected for calculating compaction. The selected Mesozoic succession is
293 more than 1000 meters thick and made up of Triassic and Jurassic sediments followed by a thin
294 Cretaceous succession. The Triassic succession (Saladilla Fm: Jabaloy-Sánchez *et al.* 2019)
295 comprises four levels (T1 to T4) consisting of continental redbeds with calcareous and

296 conglomeratic intercalations belonging to shallow marine-transitional and continental realms.
297 At the end of the Triassic succession, conformably the Jurassic succession (Castillón Fm:
298 Jabaloy-Sánchez et al. 2019) appears. This is a shallow marine succession (J1 to J3) with three
299 levels made of dolostones, at the base, followed by several limestone facies evolving upward to
300 nodular limestones at the Late Jurassic. The thin Cretaceous succession (C1) shows limestones
301 appearing in continuity over the Late Jurassic succession, sandy glauconite-rich marls and
302 marly-limestones and marls at the top. The Mesozoic succession is followed, after an
303 unconformity, by a thick (close to 1700 m) Tertiary succession composed of several carbonate
304 and marly formations (E1 to E3: Mula, Valdelaparra, España, Malvariche, Cánovas and As
305 Fms; and O1-O2: El Bosque Fm: Jabaloy-Sánchez et al. 2019) evolving from shallow marine
306 (during the Paleogene) to deep marine realms in the Early Miocene (M1A to M1C: Río Pliego
307 and El Niño Fms: Jabaloy-Sánchez et al. 2019). It is believed that, after M1C was deposited,
308 exhumation began in the area and no more deposits took place in the area (see below).
309 In the Early Oligocene, a tectonic phase took place and the tectonic Perona Unit (PU) appears
310 thrusting on the Lowermost Oligocene Succession and is unconformably covered by the rest of
311 the Succession (Oligocene and Early Miocene).
312 In this succession a mineralogical, petrographical and geochemical study was performed on the
313 Triassic redbeds by Perri *et al.* (2013). Illite crystallinity values, illitization of kaolinite,
314 occurrence of typical authigenic minerals and apatite fission-track studied suggested burial
315 depths of the base of the Triassic succession of 4 to 6 km with temperatures of 140-160 °C,
316 typical of the burial diagenetic stage. The exhumation of the succession was also dated at 15.6
317 Ma (Early Langhian) when a rapid cooling below the 110 °C isotherm took place.

318

319

----- Figure 1 -----

320

321 **4. Result of calculating**

322 *4.1. Porosity-depth change (traditional method)*

323 For the calculations of the original thickness two curves have been used (Fig. 2, Table 2): from
324 Steckler and Watts (1978) and from Bond *et al.* (1983). With the curve from Steckler and Watts
325 (1978) the original porosity in all the cases is close to 55 % of the whole rock and the end
326 porosity range from 8 to 54 % according to the depth (Table 1). In the case of the curves from
327 Bond *et al.* (1983) a set of double exponential lithology-dependent curves appear with a low-
328 and upper limits of compaction of the same lithology. If the set of lower-limit curves is taken
329 into account (an early cementation is assumed) the original porosities range from 20 to 55 %,
330 and the end porosities range from 2 to 29 % of the whole rock depending on the lithology and
331 the depth (Table 1).

332

333 ----- Figure 2 -----

334

335 ----- Table 1 -----

336

337 With the curve from Steckler and Watts (1978) the whole succession (thickness of 3025 m),
338 becomes 4863 m thick when decompaction is performed (Fig. 3). It presents a thickness
339 reduction of 1838 m. This curve provides a high degree of compaction in deeper levels, while
340 progressively decreasing in shallow levels. In deep levels, in most cases, the thickness becomes
341 double if compared to the measured.

342 In the case of the calculations with the set of lower-limit curves from Bond *et al.* (1983) the
343 whole succession becomes 4012 m thick (Fig. 3) after decompaction (thickness reduction of 987
344 m). With these lower-limit curves the sedimentary sequences made of soft sediments (silts,
345 clays, marls, sands and gypsums) became compacted in a high degree (even more than with the
346 curve of Steckler and Watts, 1978). This can be seen in the soft Triassic (T2) sequence with 100
347 m measured becoming 207 m thick after decompaction. Contrary, sequences with hard
348 lithologies (carbonates, conglomerates, etc) appear with less compaction since they are thought
349 to undergo early cementation. This is the case of the hard Jurassic (J1) sequence with 125 m
350 thickness measured in the field, and with an original thickness of only 158 m.

351 When the mean values are obtained with both former estimations, the whole succession
352 becomes 4441 m thick (Fig. 3; Table 1) after decompaction. It implies a thickness reduction of
353 1416 m.

354

355 ----- Figure 3 -----

356

357 4.2. Elastic by Steinbrenner

358 The results (Fig. 3, Table 2) indicate that the whole succession (3025 m) becomes 3631 m (a
359 thickness reduction of 606 m). This method does not show perceptible differences among hard
360 and soft lithologies after compaction. So, the soft Triassic sequence (700 m) becomes 923 m
361 thick, while the also soft Eocene sequence (275 m) becomes 416 m in origin. The hard-Jurassic
362 sequence (325 m) shows an original thickness of 386 m. The Oligocene sequence together with
363 the Perona Unit (1250 m) changes to 1387 m in origin. The Early Miocene is 450 m thick and it
364 becomes only 481 m after decompaction.

365

366 ----- Table 2 -----

367

368 4.3. Oedometric

369 The results (Fig. 3, Table 3) indicate that the whole succession (3025 m) becomes 3811 m
370 (thickness reduction of 786 m). This method does not show perceptible differences in
371 compaction values between hard and soft lithologies. So, the soft Triassic sequence (700 m)
372 becomes 820 m thick and the soft Eocene one (275 m) becomes 305 m in origin. The hard-
373 Jurassic sequence (325 m) shows an original thickness of 345 m. The Early Miocene is 450 m
374 thick and it becomes 493 m after decompaction. Nevertheless, a high compaction is observed in
375 the thicker levels such as the Oligocene sequence together with the Perona Unit (1250 m)
376 changing to 1822 m in origin.

377

378

----- Table 3 -----

379

380 *4.4. Change of specific weight of the sediment*

381 The results (Fig. 3, Table 4) indicate that the whole succession (3025 m) becomes 4020 m
382 (thickness reduction of 995 m). Soft lithologies are compacted more than hard sediments. The
383 Triassic sequence (700 m) becomes 982 m thick and the Eocene one (275 m) becomes 380 m in
384 origin. The Jurassic sequence, which is made of hard carbonates (325 m), shows an original
385 thickness of 469 m. The Oligocene sequence, made of hard carbonates and conglomerates,
386 together with Perona Unit, which is also made of previously consolidated carbonates, change
387 from 1250 m measured today to 1561 m in origin, by the loading of soft sediments from the thin
388 Early Miocene sequence. The Early Miocene is 450 m thick and it becomes only 595 m after
389 decompaction.

390

391

----- Table 4 -----

392

393 *4.5. Loadcap program*

394 The results, shown in Table 5 and Figure 3, indicate that the whole succession (3025 m)
395 becomes 4117 m. It shows a thickness reduction of 1092 m. In a similar way to the former
396 calculations, soft lithologies suffer greater compaction than hard sediments. So, the Triassic
397 sequence (700 m) becomes 1125 m thick after decompaction and the Eocene one (275 m)
398 becomes 536 m in origin. The Jurassic sequence, made of hard carbonates (325 m), shows an
399 original thickness of about 412 m. The hard Oligocene sequence together with the Perona Unit
400 (1250 m) change to 1488 m in origin since a minor loading due to soft sediment from the thin
401 early Miocene sequence took place. The Early Miocene sequence was deeper and a water
402 column of 500 m was considered in the calculations. In this case, the sequence is 450 m thick
403 and it becomes only 513 m after decompaction.

404

405

----- Table 5 -----

406

407 **5. Discussion**

408 The results obtained from all the above calculations (Fig. 4) indicate that the higher compaction
409 (37.8 %) is obtained with the porosity-depth change methods from Steckler and Watts (1978).

410 Nevertheless, the most restrictive porosity-depth change method from Bond *et al.* (1983) using

411 the lower-limit curves implies a compaction of 24.6 % for the studied succession (Fig. 4, Table

412 6). The mean value for the porosity-depth change methods provides a compaction of 31.2 %

413 (Fig. 4). The alternative methods used for calculating compaction in the same succession (Fig.

414 4, Table 6), have provided a compaction rank from 16.7 % using the elastic method by

415 Steinbrenner to 26.5 % using the Loadcap program, with intermediate values of 20.6 % using

416 the oedometric method and 24.7 % using the specific weight method. When the mean of all

417 methods is calculated a compaction of about 25 % is obtained. The value of 24.6 % obtained

418 with the porosity-depth change method from Bond *et al.* (1983) using the lower-limit curves is

419 within the average of the values obtained with the alternative methods. The standard deviation

420 of the initial thicknesses is 195 m, while the variation coefficient is 5 %.

421

422

----- Figure 4 -----

423

424

----- Table 6 -----

425 **5.1. Implications according to sediment lithology**

426 When the results of compaction are taken into account separately for hard versus soft rocks, and

427 for thick versus thin beds, some interesting assessments can be extracted (Fig. 4, Table 6). In the

428 case of hard rocks, such as the carbonate Jurassic part of the succession, the highest value for

429 compaction (44.5 %) is obtained with the porosity-depth change method by Steckler and Watts

430 (1978). A compaction of 20.7 % is obtained with the variety from Bond *et al.* (1983) with the

431 lower-limit curves. This value is comparable with the intermediate values obtained through the

432 alternative methods. When the alternative methods proposed in this paper are compared, the
433 specific weight method (30.7 %) provides higher values for the compaction of hard rocks. In
434 contrast, the oedometric method (5.9 %) gives lower value; meanwhile intermediate values are
435 obtained with the elastic by Steinbrenner (15.9 %) and Loadcap software (21.1 %) methods. If
436 soft sediments, such as the Eocene part of the succession, are considered, the upper value (48.7
437 %) is obtained with the alternative Loadcap software method. The values for the compaction
438 obtained with the porosity-depth change methods are: 41.4 % with the method from Steckler
439 and Watts (1978) and 37.4 % with the method from Bond *et al.* (1983) with the lower-limit
440 curves. In the case of the other alternative methods proposed in this paper, the Loadcap software
441 value (48.7 %) is followed, from upper to lower, by the elastic method by Steinbrenner (33.9
442 %), specific weight method (27.6 %) and the oedometric method (9.8 %).

443

444 5.2. Implications according to the thickness of the beds

445 When a thick sequence, such as the Lower Oligocene part of the succession, is analyzed, high
446 values for compaction are obtained with the oedometric method (40.4 %). In the case of the
447 porosity-depth change method 14.0 % is obtained with the lower-limit curves from the Bond *et*
448 *al.*, (1983) method, and 35.7 % with the method from Steckler and Watts (1978). When the
449 alternative methods are compared from greatest to least, the oedometric method (40.4 %) is
450 followed by the specific weight method (23.5 %), Loadcap software (18 %) and elastic by
451 Steinbrenner (9.4 %). In the case of a thin sequence, such as the Cretaceous part of the
452 succession, higher values for compaction are obtained again with the porosity-depth change
453 method (49 % with lower-limit curves from the method from Bond *et al.*, 1983; 43.2 % with the
454 method from Steckler and Watts, 1978). When the alternative methods proposed in this paper
455 are compared, the Loadcap software (41.9 %) method provides higher values for the
456 compaction. Otherwise, the oedometric method (3.8 %) gives lower value; meanwhile
457 intermediate values are obtained with the elastic by Steinbrenner (32.2 %) and the Specific
458 Weight (25.1 %) methods.

459 In general, similar values for compaction (but with a certain variability) are obtained using the
460 alternative methods (Fig. 4) and in the same range of values obtained with the lower-limit
461 curves from the method from Bond *et al.*, (1983). Nevertheless, some further constraints could
462 be introduced due to the results of mineralogical studies performed by Perri *et al.* (2013) in the
463 same stratigraphic succession of the study area. These studies, composing illite crystallinity
464 values, illitization of kaolinite, occurrence of typical authigenic minerals and apatite fission-
465 track, indicated a burial depth of the base of the Triassic succession of 4 to 6 km deep, with
466 temperatures of 140-160 °C (typical of the burial diagenetic stage). Taking this into account, the
467 most plausible alternative methods could be the Loadcap program calculations (4117 m of
468 original thickness), and the specific weight (4020 m of original thickness). Both methods are
469 close to the value obtained with the lower-limit curves from the method from Bond *et al.*,
470 (1983). So, these three methods appear inside but close to the lower limit proposed by Perri *et*
471 *al.* (2013) of the 4000 m of depth. Moreover, the specific weight change method provides the
472 initial thickness with the inputs of the final thickness and the initial and final specific weights of
473 each stratigraphic level, being a method based in similar principles to that of the porosity
474 method, but with the input of the specific weight, which is a parameter much less variable to the
475 porosity, and much easier and quicker to obtain.

476 Otherwise, the compaction results obtained using the oedometric method and elastic method by
477 Steinbrenner were below the minimum compaction required by mineralogical data from Perri *et*
478 *al.* (2013). The elastic method by Steimbrenner provided the lowermost value for compaction of
479 the whole succession (Fig. 4). This method provides very low values for compaction of hard
480 rocks (Jurassic, Lower Oligocene and Perona Unit). In the case of these hard rocks, it is evident
481 that cementation and diagenesis took place. On the contrary, this method seems to be much
482 more adapted to soft clay and marl dominant sediments (Fig. 4). The constraints of the elastic
483 method imply that compaction mainly accounts for the consolidated sediments. The possible
484 compaction for unconsolidated sediments is assumed as negligible by this method.

485 On the other hand, the oedometric method provides the lowermost values of compaction for
486 both hard and soft rocks. It also seems to be greatly influenced by the thickness of the

487 considered beds, presenting higher compaction in thicker beds and lower in thin ones (Fig. 4).
488 This is due to the intrinsic constraints of the method: (1) the main compaction in the
489 unconsolidated stage; (2) the compaction is due to the thickness and weigh of the bed itself. The
490 intrinsic constraints of the main compaction in the unconsolidated stage is in accordance to that
491 proposed by Fowler and Yang (1998, 1999), Yang (2001), Cheauveau and Kaminski (2008) and
492 Stefaniuk and Mackowski (2000), but regardless of that, it does not seem that compaction could
493 only be due to the intrinsic weigh of the bed since overlaying beds should be also responsible
494 for part of the compaction.

495

496 5.3. Implications when intra thrust systems take place

497 An important feature of the studied stratigraphic succession is the presence of a thrusting nappe
498 (Perona Unit) intercalated in the succession at the Oligocene level. This can be a frequent
499 situation in old sedimentary basins that usually are not taken into account in compaction studies.
500 In fossil sedimentary basin is frequent this situation and also other tectonic perturbations as
501 folds and faults. The influence of folding and faulting can easily be eliminated by restoring and
502 balancing, so that, not affecting for compaction calculations. Nevertheless, a thrusting is a very
503 influential element in compaction since induces an overload on the underlying succession (also
504 could undergo its own compaction). When the compaction results from different methods are
505 compared for this thrusting unit (Fig. 4, Table 6), high values are obtained with the porosity-
506 depth change methods (15 % with the lower-limit curves by Bond *et al.*, 1983; 39.1 % with the
507 method by Steckler and Watts, 1978). Those results are probably due to the fact that porosity-
508 depth change methods do not take into account that the sediments of a tectonic unit have already
509 been compacted due to the overlaying succession prior to the structuring in Oligocene times. In
510 the case of comparing the alternative methods proposed in this paper, the lower (no or minimal)
511 compaction are obtained with the specific weight (0.0 %) and Loadcap software methods (2.9
512 %) because these methods consider that sediments were already compacted prior to the
513 emplacement of the tectonic unit. Intermediate (but low) similar values are obtained with the
514 oedometric (6.9 %) and elastic by Steimbrenner (7.4 %) methods considering a low compaction

515 due to the load of the overlaying Miocene part of the succession. The specific weight and
516 Loadcap software methods seem to be more accurate for the compaction of the thrusting unit
517 since null or very low values for compaction are obtained, because those sediments were
518 already compacted prior to the structuring.

519

520 **6. Conclusions**

521 - Alternative methods based on physical calculation (elastic by Steinbrenner, oedometric and
522 change of the specific weight of the sediment) and geotechnical and engineering software
523 (Loadcap software) are introduced to calculate compaction in the Meso-Cenozoic marine
524 succession cropping out in the Sierra Espuña area (SE Spain).

525 - The inputs used for calculations (physical properties, coefficients and modules) are standards
526 derived from literature, real data coming from engineering-geotechnical studies, and thicknesses
527 measured in the field; but in all methods those inputs are the same allowing a valid comparison
528 (Fig. 5).

529

530 ----- Figure 5 -----

531

532 - The evidence presented in this paper, indicate that compaction resulting from the application
533 of alternative methods in old sedimentary basins are comparable with that obtained with the
534 lower-limit curves of the traditional porosity-depth change methods (Fig. 5).

535 - The constraints of mineralogical studies in the same studied area (Perri *et al.*, 2013) suggest
536 that compaction obtained with the specific weight method and the Loadcap program could be
537 the more accurate of that alternative new methods (Fig. 5).

538 - Moreover, in the case of the specific weight method, it seems that it is the least affected
539 method by the lithological type, being as valid for hard (cemented) as for soft rocks (Fig. 5).

540 - The elastic (Steimbrenner) method provided excessively low values for compaction of hard
541 rocks because it considers that compaction only occurs in the consolidated stage and disregards

542 the latest possible compaction in unconsolidated one. Apart from that, it seems to be much more
543 applicable to soft rocks (Fig. 5).

544 - The oedometric method seems to be a method greatly influenced by the thickness of the
545 considered beds providing higher compactations in thicker beds and lower in thin ones (Fig. 5).

546 This is due to the inherent constraints of the method regarding the assumption that compaction
547 is due to the thickness and weigh of the bed itself in the unconsolidated stage, while
548 disregarding the possible compaction due to overlaying beds in the consolidated stage.

549 - The particularity of the occurrence of a thrusting unit in the succession (very common in old
550 sedimentary basins) is also studied. The effect of the loading in the underlying succession and
551 the compaction of this unit have also been studied indicating that the specific weight and
552 Loadcap software methods are the most appropriate (Fig. 5), because these methods consider
553 that the sediments of this thrusting unit were mainly compacted prior to the tectonic
554 emplacement.

555

556 **Acknowledgements**

557 Research supported by: CGL2016-75679-P research project (Spanish Ministry of Education and
558 Science); Research Groups and projects of the Generalitat Valenciana from Alicante University
559 (CTMA-IGA). Comments and corrections performed in a former version of the manuscript by
560 M. Kominz are much appreciated. Company Esfera Consultores de Construcción is also
561 acknowledged by the geotechnical support.

562

563

564 **References**

565 Allen, P.A., Allen, J.R., 1990. Basin Analysis: *Principles and Applications*: Oxford (Blackwell
566 Sci. Publ.).

567 Atkinson, J., 2007. The Mechanics of Soils and Foundation. Second Edition by Taylor &
568 Francis. Abingdon, Oxon, OX14 4RN.

- 569 Barnes, G. E., 2000. *Soil Mechanics: Principles and Practice*. Second Edition by Palgrave
570 Macmillan. Hampshire RG21 6XS.
- 571 Benjamin, U.K., Nwachukwu, J.I., 2011. Model compaction equation for hydrostatic sandstones
572 of the Niger Delta. *Ife Journal of Science*, 13 (1), 161-174.
- 573 Bjorlykke, K., 2014. Relationships between depositional environments, burial history and rock
574 properties. Some principal aspects of diagenetic processes in sedimentary basins.
575 *Sedimentary Geology*, 301, 1-14.
- 576 Bond, G.C. and Kominz, M.A., 1984. Construction of tectonic subsidence curves for the early
577 Paleozoic miogeocline, southern Canadian Rocky Mountains: Implications for subsidence
578 mechanisms, age of breakup, and crustal thinning. *Geological Society of America Bulletin*,
579 95 (2), 155-173.
- 580 Bond, G.C., Kominz, M.A., Devlin, W.J., 1983. Thermal subsidence and eustasy in the lower
581 Paleozoic miogeocline of western North America. *Nature*, 306, 775-779.
- 582 Cheauveau, B., Kaminski, E., 2008. Porous compaction in transient creep regime and
583 implications for melt, petroleum, and CO₂ circulation. *Journal of geophysical research*, 113,
584 doi:10.1029/2007JB005088.
- 585 Critelli, S., 2018. Provenance of Mesozoic to Cenozoic circum-Mediterranean sandstones in
586 relation to tectonic setting. *Earth Sci. Reviews* 185, 624-648.
- 587 Critelli, S., Mongelli, G., Perri, F., Martín-Algarra, A., Martín-Martín, M., Perrone, V.,
588 Zaghoul, M.N., 2008. Compositional and geochemical signatures for the sedimentary
589 evolution of the Middle Triassic-Lower Jurassic continental redbeds from Western-Central
590 Mediterranean Alpine Chains. *Journal of Chicago*, 116, 375-386.
- 591 Feiner, A., Lehnert, J., Lohr, A., 1976. Asphaltic concrete core problems and their solutions.
592 *Transactions, 12th Int. Congress on Large Dams 1976; R.3 - Q.44*, 33– 47.
- 593 Fowler, A.C., Yang, X.S., 1998. Fast and slow compaction in sedimentary basins. *SIAM Journal*
594 *of Applied Mathematics*, 59, 365-385.
- 595 Fowler, A.C., Yang, X.S., 1999. Pressure solution and viscous compaction in sedimentary basins,
596 *Journal of geophysical research*, 104 (86), 12989-12997.

- 597 Gabasova, L.R., Kite, S. (2018) Compaction and sedimentary basin analysis on Mars. *Planetary*
598 *and Space Science*, 152, 86-106.
- 599 González de Vallejo, L.I., 2002. *Ingeniería Geológica*. Editorial Pearson Educación (Madrid).
600 715 pp.
- 601 Grundbau-Taschenbuch, 1980. 3ª Ed. 1ª Parte Wilhelm Ernst & Sohn, Berlin.
- 602 Guerrero, F., Martín-Algarra, A., and Perrone, V., 1993, Late Oligocene-Miocene syn- /-late-
603 orogenic successions in Western and Central Mediterranean Chains from the Betic
604 Cordillera to the Southern Apennines. *Terra Nova*, v. 5, p. 525-544.
- 605 Jiménez-Salas, J.A. et al., 1975. *Propiedades de los suelos y de las rocas (Geotecnia y*
606 *Cimientos I)*. Editorial Rueda (Madrid). 466 pp.
- 607 Jabaloy-Sánchez, A., Martín-Algarra, A., Padrón-Navarta, J.A., Martín-Martín, M., Gómez-
608 Pugnaire, M.T., López-Sánchez-Vizcaíno, V. Garrido, C.J., (2019). Lithological successions
609 in the Internal Zones and Flysch Trough units of the Betic Chain, 377-432. In: *The Geology*
610 *of Iberia: a Geodynamic Approach*. Quesada and Oliveira Eds. Springer Nature
611 Switzerland.
- 612 Jiménez-Salas, J.A. et al., 1980. *Mecánica del suelo y de las rocas (Geotecnia y Cimientos II)*.
613 Editorial Rueda (Madrid). 1188 pp.
- 614 Kominz, M.A., Patterson, K., Odette, D., 2011. Lithology dependence of porosity in slope and
615 deep marine sediments. *Journal of Sedimentary Research*, 81, 730-742.
- 616 Marcussen, O., 2009. *Compaction of siliceous sediments: implications for basin modeling and*
617 *seismic interpretation*. Ph Thesis University of Oslo (Norway), 160 pp.
- 618 Marcussen, O., Thyberg, B.I., Peltonen, C., Jahren, J., ; Bjørlykke, K., Faleide, J.I., 2009.
619 *Physical properties of Cenozoic mudstones from the northern North Sea: Impact of clay*
620 *mineralogy on compaction trends*. *AAPG Bulletin*, 93 (1), 127-150.
- 621 Martín-Martín, M., Martín-Algarra, A., 2002. Thrust sequence and syntectonic sedimentation in
622 a piggy-back basin: the Oligo-Aquitania Mula-Pliego Basin (Internal Betic Zones, SE
623 Spain). *Comptes Rendus Geosciences*, 334, 363-370.

- 624 Martín-Martín, M., El Mamoune, B., Martín-Algarra, A., Martín-Pérez, J.A., Serra-Kiel, J.,
625 1997. Timing of deformation in the Malaguide Complex of the Sierra Espuña (SE Spain).
626 *Geologie en Mijnbouw*, 75, 309-316..
- 627 Martín-Martín, M., Martín-Rojas, I. Caracuel, J.E., Estévez-Rubio, A., Martín-Algarra, A.,
628 Sandoval, J., 2006a. Tectonic framework and extensional pattern of the Malaguide Complex
629 from Sierra Espuña (Internal Betic Zone) during Jurassic-Cretaceous: implications for the
630 Westernmost Tethys geodynamic evolution. *International Journal of Earth Sciences*, 95,
631 815-826.
- 632 Martín-Martín, M., Sanz de Galdeano, C., García-Tortosa, F.J., Martín-Rojas, I., 2006b.
633 Tectonic units from the Sierra Espuña-Mula área (SE Spain): implication on the triassic
634 paleogeography and geodynamic evolution for the Betic-Rif internal zone. *Geodinamica*
635 *Acta*, 19, 1-9.
- 636 Mayer, L., 1987. Subsidence analysis of the Los Angeles Basin, In: “Cenozoic basin
637 development of coastal California” (Ingersoll et al. Eds). Prentice-Hall, Englewood Cliffs,
638 New Jersey, 299-320.
- 639 Meckel, T.A., Ten Brink, U.S., Williams, S.J., 2006. Current subsidence rates due to
640 compaction of Holocene sediments in southern Louisiana. *Gephysical Research Letters*, 33,
641 doi: 10.1029/2006GL026300.
- 642 Meckel, T.A., Ten Brink, U.S., Williams, S.J., 2007. Sediment compaction rates and subsidence
643 in deltaic plains: numerical constraints and stratigraphic influences. *Basin Research*, 19, 19-
644 31.
- 645 Ministerio de Fomento, 2009. Guía de cimentaciones en obras de carreteras. Series
646 Monográficas. 3ª Edición revisada.
- 647 NAVFAC DM 7-1, 1986. Soil Mechanics, Design Manual, 7.1.
- 648 NAVFAC DM 7-2, 1986. Foundations and Earth Structures, Design Manual, 7.2.
- 649 Perri, F. Critelli, S., Martín-Algarra, A., Martín-Martín, M., Perrone, V., Mongelli, G., Zattin,
650 M., 2013. Triassic redbeds in the Malaguide Complex (Betic Cordillera – Spain):

- 651 pegrography, geochemistry and geodynamic implications. *Earth Sci. Reviews*, 117 (15), 1-
652 28.
- 653 Perri, F. Critelli, S., Martín-Martín, M., Montone, S., Amendola, U., 2017. Unravelling
654 hinterland and offshore palaeogeography from pre-to-syn-orogenic clastic sequences of the
655 Betic Cordillera (Sierra Espuña), Spain. *Palaeogeography, Palaeoclimatology,*
656 *Palaeoecology*, 468 (15), 52-69.
- 657 Poelchau, H.S., Baker, D.R., Hantschel, T., Horsfield, B., Wygrala, B., 1997. Basin Simulation
658 and the Design of the Conceptual Basin Model. In: "Petroleum and basin evolution" (Welte,
659 D.H. et al. Eds.), 3-70.
- 660 Roberts, A.M., Kusznir, N.J., Yielding, G., Styles, P., 1998. 2D flexural backstripping of
661 extensional basins: the need for a sideways glance. *Petroleum Geoscience*, 4, 327-338.
- 662 Rodríguez Ortiz, J.M. et al., 1995. Curso aplicado de cimentaciones. Servicio de publicaciones
663 del Colegio Oficial de Arquitectos de Madrid. 6ª Edición corregida y aumentada. 267 pp.
- 664 Schleicher, F., 1926. Zur theorie des Baugrundes. *Bauingenieur*. 7: 931-936.
- 665 Schneider, F., Potdevin, J.L., Wolf, S., Fraille, I. 1996. Mechanical and chemical compaction
666 model for sedimentary basin simulators. *Tectonophysics*, 263, 307-317.
- 667 Sclater, J.G., Christie, P.A.F., 1980. Continental stretching: an explanation in the Northern
668 Viking Graben. *Journal of the Geological Society of London*, 152, 15-26.
- 669 Steckler, M.S., Watts, A.B., 1978. Subsidence of the Atlantic-type continental margin of New
670 York: *Earth and Planetary Science Letters*, 41, 1-13.
- 671 Stefaniuk, M., Mackowski, T., 2000. A compacted thickness correction in the paleotectonic
672 reconstruction. *Geological Quarterly*, 44 (1), 101-108.
- 673 Steinbrenner, W., 1936. A rational method for the Determination of the vertical Normal Stresses
674 under Foundations. 1° ICOSOMEF, Harvard, 2: 142-143.
- 675 Suetnova, E., Vasseur, G. 2000. 1-d modelling rock compaction in sedimentary basins using a
676 visco-elastic rheology. *Earth Planetary Science Letters*, 178, 373-383.
- 677 Terzaghi, K., Peck, R., 1976. *Soil Mechanics in Engineering Practice*. Second Edition by John
678 Wiley & Sons, Inc. New York.

- 679 Van Hinte, J.E., 1978. Geohistory analysis: application of micropaleontology in exploration
680 geology. *American Association of Petroleum Geologist Bulletin*, 62, 201-222.
- 681 Van Sickel, W.A., Kominz, M.A., Miller, K.G., Browning, J.V., 2004. Late Cretaceous and
682 Cenozoic sea-level estimates: backstripping analysis of borehole data, onshore New Jersey.
683 *Basin Research*, 16, 451-465.
- 684 Wagreich, M., Schmid, H.P., 2002. Backstripping dip-slip fault histories: apparent slip rates for
685 the Miocene of Vienna Basin. *Terra Nova*, 14, 163-168.
- 686 Watts, A.B., 1978. An analysis of isostasy in the world's oceans 1. Hawaiian-Emperor
687 seamount chain. *Journal of Geophysical Research: Solid Earth*, 83 (12), 5989-6004.
- 688 Watts, A.B., 1981. The U.S. Atlantic continental margin: subsidence history, crustal structure
689 and thermal evolution, In: "Geology of passive continental margins: history, structure and
690 sedimentologic recor" Bally et al. Eds. Special vol. of American Association of Petroleum
691 Geologist, 19. 75 pp.
- 692 Watts, A.B., Ryan, W.B.F., 1975. Flexure of the lithosphere and continental margin basins.
693 *Tectonophysics*, 36, 25-44.
- 694 Yang, X.S., 2001. A unified approach to mechanical compaction, pressure solution, mineral
695 reactions and the temperature distribution in hydrocarbon basins. *Tectonophysics*, 330,
696 141-141.

697

698 Figure caption

699

700 **Figure 1.-** A) location of the key-case study area in Sierra Espuña, Murcia province (SE,
701 Spain); B) geological map and section of the Sierra Espuña area.

702 **Figure 2.-** Graphics with the calculations of the porosity-depth change of sediment according to
703 Steckler and Watts (1978) and to Bond *et al.* (1983). In the case of Bond *et al.* (1983) only
704 the set of lower-limit curves have been used for calculating compaction.

705 **Figure 3.-** Accumulate thickness-age (My) graphic with the comparative of the measured
706 thickness and the results of original accumulate thickness along time of the studied

707 succession after decompaction with the whole methods. The mean thickness with the whole
708 methods is also represented with dash line. Key: ESM: elastic by Steinbrenner; SWM:
709 specific weight of the sediment methods; OM: oedometric method; PCM: porosity change
710 method (Bond et al., 1983); LSM: use of Loadcap software method.

711 **Figure 4.-** Histograms with the % of compaction of the whole succession, Jurassic hard rocks,
712 Eocene soft rocks, thicker Lower Oligocene, thinner Cretaceous and the thrusting Perona
713 Unit.

714 **Figure 5.-** Comparative of the compaction (%) according all the methods for the whole
715 succession; for the hardest, the softer, the thicker and the thinner intervals; and for the
716 thrusting unit.

717 .

718

719 **Table caption**

720

721 **Table 1.-** Results of the compaction calculating with the porosity-depth change method.

722 **Table 2.-** Results of the compaction calculating with the elastic by Steinbrenner method.

723 **Table 3.-** Results of the compaction calculating with the oedometric method.

724 **Table 4.-** Results of the compaction calculating with the specific weight change method.

725 **Table 5.-** Results of the compaction calculating with the Loadcap software method.

726 **Table 6.-** Synthesis of the results of the compaction calculating with the whole methods.

Stratigraphic Unit	Lithology (age)	Thickness	Accumulated	Original Porosity thick Steckler & Watts (1978)	Final Porosity	Original thick Bond et al. (1983)	Original Porosity	Final Porosity	Original	Mean value
Río Pliego and El Niño Fms (450 m)	M1C.- marls and siliceous marls (Burdigalian)	100 m	100	55%	54%	102	30%	29%	101	102
	M1B.- conglomerates (Late Aquitanian)	200 m	300	55%	50%	222	25%	22%	208	215
	M1A.- marls and sandstones (Early Aquitanian)	150 m	450	55%	47%	177	55%	27%	243	210
El Bosque Fm (950 m)	O2.- marls (Late Oligocene)	200 m	650	55%	42%	258	55%	25%	333	296
	O1.- conglomerados y carbonatos (Early Oligocene)	750 m	1400	55%	31%	1167	20%	7%	872	1020
Perona Thrusting Unit	PU.- dolostones and limestones (Liassic)	300 m	1700	55%	26%	493	20%	6%	353	423
Espuña, Valdelaparra, Malvariche, Cánovas and As Fms (275 m)	E3.- marls (Late Lutetian-Earliest Oligocene)	100 m	1800	55%	23%	164	55%	13%	193	179
	E2.- clays (Early Lutetian)	50 m	1850	55%	22%	86	55%	12%	98	92
	E1.- Calcarenites (Ypresian)	125 m	1975	55%	21%	219	20%	5%	148	184
Cretaceous (25 m)	C1.- limestones, marly limestone and sands (Cretaceous)	25 m	2000	55%	21%	44	55%	11%	49	47
Castillón Fm (350 m)	J3.- nodular limestones (Malm)	75 m	2075	55%	20%	133	25%	6%	94	114,0
	J2.- Limestones and marlylimestones (Dogger)	125 m	2200	55%	19%	225	25%	5%	158	192
	J1.- Dolostones (Liassic)	125 m	2325	55%	18%	228	25%	5%	158	193
Saladilla Fm (700 m)	T4.- clays with gypsum (Norian-Raethian)	25 m	2350	55%	14%	48	55%	9%	51	49
	T3.- limestones (Carnian)	375 m	2725	55%	12%	733	25%	3%	485	609
	T2.- clays, sands and sandstones (Ladinian)	100 m	2825	55%	10%	200	55%	7%	207	203
	T1.- conglomeres and sands (Scitayan)	200 m	3025	55%	8%	364	25%	2%	261	313
Total original thickness						4863			4012	4441
Total thickness reduction						1838			987	1416

Table 1

Thickness	Accumulated	Unconsolidated sediments compaction (UC)				Consolidated sediments compaction (CC)				Lithified sediments compaction (LC)			Original thickness (To)
		To fraction (%)	Compaction (m)	σ (kp/cm ²)	E (kp/cm ²)	ν	Compaction (m)	σ (kp/cm ²)	E (kp/cm ²)	ν	Compaction (m)		
		Feiner et al. (1976)				Steinbrenner, 1936				Steinbrenner, 1936			
100	100	5,000	5,5	50,0	1000	0,10	4,9	50,0	38700	0,10	0,1	110,5	
200	300	3,000	6,3	24,3	1400	0,25	2,4	24,3	44700	0,23	0,1	208,8	
150	450	4,000	6,5	74,3	1670	0,18	5,4	74,3	38700	0,17	0,2	162,1	
200	650	5,000	11,7	110,3	1000	0,10	23,1	110,3	31600	0,10	0,7	235,5	
750	1400	4,000	33,0	158,3	2120	0,24	42,9	158,3	55200	0,22	1,6	827,5	
300	1700	0,000	0,0	348,1	3300	0,23	23,3	348,1	92200	0,21	0,8	324,1	
100	1800	5,000	8,8	429,1	1000	0,10	66,8	429,1	38700	0,10	1,0	176,6	
50	1850	5,000	4,4	453,1	750	0,25	33,6	453,1	22500	0,23	0,7	88,7	
125	1975	3,000	4,5	464,1	1800	0,30	20,7	464,1	50000	0,27	0,7	150,9	
25	2000	4,000	1,5	495,3	1310	0,19	10,2	495,3	49560	0,17	0,2	36,9	
75	2075	5,000	4,4	501,5	3200	0,26	8,3	501,5	86600	0,23	0,3	88,0	
125	2200	5,000	7,4	521,3	3300	0,23	15,6	521,3	89500	0,21	0,5	148,5	
125	2325	5,000	7,5	554,4	3300	0,23	16,7	554,4	77500	0,21	0,7	149,9	
25	2350	5,000	2,4	588,1	900	0,24	19,9	588,1	25740	0,22	0,4	47,7	
375	2725	5,000	22,8	593,7	3200	0,23	57,8	593,7	67000	0,22	2,5	458,1	
100	2825	4,000	5,5	693,1	1800	0,27	31,0	693,1	43415	0,25	1,1	137,6	
200	3025	3,000	8,3	717,9	1600	0,29	69,6	717,9	45760	0,27	1,9	279,8	
Unconsolidated Total Compaction (UC):			140,5	Consolidated Total Compaction (CC):			452,2	Lithified Total Compaction (CC):			13,6		
							Total thickness reduction:	606,3				Original thickness:	3631,3

Table 2

Thickness	Accumulated	Unconsolidated Sediments Compaction (UC)			Consolidated Sediments Compaction (CC)			Lithified Sediments Compaction (LC)			Original thickness (To)		
		σ_1 (kp/cm ²)	Om (kp/cm ²)	Compactación (m)	σ_2 (kp/cm ²)	Om (kp/cm ²)	Compactación (m)	σ_3 (kp/cm ²)	Om (kp/cm ²)	Compactación (m)			
		Terzaghi, K., Peck, R., 1976			Terzaghi, K., Peck, R., 1976			Terzaghi, K., Peck, R., 1976					
100	100	12,6	228	5,8	16,8	1011	1,7	12,4	39135	0,0	107,5		
200	300	28,0	537	11,0	50,1	1527	6,8	49,3	47997	0,2	218,0		
150	450	19,1	277	11,1	68,4	1739	6,1	92,4	40096	0,3	167,5		
200	650	26,4	228	26,2	63,3	1011	13,4	135,6	31955	0,9	240,5		
750	1400	154,8	411	453,4	150,5	2298	52,6	255,3	58933	3,3	1259,3		
300	1700	54,0	> 10 ⁶	0,0	233,1	3543	21,1	390,4	97651	1,2	322,3		
100	1800	12,3	228	5,7	94,5	1011	10,3	443,1	39135	1,1	117,1		
50	1850	5,7	144	2,1	30,7	818	1,9	461,4	24160	1,0	55,0		
125	1975	13,1	308	5,5	24,7	2066	1,5	479,9	55547	1,1	133,1		
25	2000	3,1	253	0,3	28,1	1370	0,5	495,3	51396	0,2	26,0		
75	2075	9,6	299	2,5	16,0	3522	0,3	508,3	92988	0,4	78,3		
125	2200	16,2	344	6,2	36,6	3543	1,3	534,8	94792	0,7	133,2		
125	2325	16,2	344	6,2	50,2	3543	1,8	568,3	82082	0,9	133,9		
25	2350	2,7	140	0,5	36,8	974	1,0	588,1	27481	0,5	27,0		
375	2725	55,1	344	71,4	56,4	3436	6,3	641,1	71432	3,4	456,1		
100	2825	11,4	264	4,5	112,4	2000	6,0	702,8	47165	1,5	112,0		
200	3025	26,7	355	16,2	49,0	1815	5,5	739,0	50936	2,9	224,6		
Total Unconsolidated Compaction (UC):				628,6	Total Consolidated Compaction (CC):				138,0	Total Lithified Compaction (LC):			19,7
Total thickness reduction:				786,4								Original thickness:	3811,4

Table 3

Stratigraphic Unit	Lithology (age)	Thickness	Accumulated	Specific Weight (T/m ³)		Original thickness (T ₀)
				Unconsolidated	Consolidated	
Grundbau-Taschenbuch, 1980; NAVFAC DM 7-1 y 7-2, 1986 and others $H_0 = H_f \frac{\gamma_f}{\gamma_0}$						
Río Pliego and El Niño Fms (450 m)	M1C.- marls and siliceous marls (Burdigalian)	100 m	100	1,78	2,48	139,3
	M1B.- conglomerates (Late Aquitanian)	200 m	300	1,99	2,45	246,2
	M1A.- marls and sandstones (Early Aquitanian)	150 m	450	1,78	2,48	209,0
El Bosque Fm (950 m)	O2.- marls (Late Oligocene)	200 m	650	1,75	2,45	280,0
	O1.- conglomerados y carbonatos (Early Oligocene)	750 m	1400	1,93	2,53	981,1
Perona Thrusting Unit	PU.- dolostones and limestones (Liassic)	300 m	1700	2,70	2,70	300,0
España, Valdelaparra, Malvariche, Cánovas and As Fms (275 m)	E3.- marls (Late Lutetian-Earliest Oligocene)	100 m	1800	1,75	2,45	140,0
	E2.- clays (Early Lutetian)	50 m	1850	1,64	2,40	73,2
	E1.- Calcarenites (Ypresian)	125 m	1975	1,50	2,00	166,7
Cretaceous (25 m)	C1.- limestones, marly limestone and sands (Cretaceous)	25 m	2000	1,81	2,42	33,4
Castillón Fm (350 m)	J3.- nodular limestones (Malm)	75 m	2075	1,85	2,65	107,4
	J2.- Limestones and marlylimestones (Dogger)	125 m	2200	1,85	2,65	179,1
	J1.- Dolostones (Liassic)	125 m	2325	1,85	2,70	182,4
Saladilla Fm (700 m)	T4.- clays with gypsum (Norian-Raethian)	25 m	2350	1,59	2,36	37,1
	T3.- limestones (Carnian)	375 m	2725	1,85	2,65	537,2
	T2.- clays, sands and sandstones (Ladinian)	100 m	2825	1,63	2,46	150,9
	T1.- conglomeres and sands (Scythian)	200 m	3025	1,85	2,37	256,8
Original thickness:						4019,8
Final thickness:						3025,0
Total thickness reduction:						994,8

Original thickness (T₀), final thickness (H_f), unconsolidated specific weight (γ₀) and consolidated specific weight (γ_f)

Table 4

Stratigraphic Unit	Levels	Measured Thickness	Corrected thickness	Back-strip. 1	Back-strip. 2	Back-strip. 3	Back-strip. 4	Back-strip. 5	Back-strip. 6	Back-strip. 7	Back-strip. 8	Back-strip. 8	Back-strip. 10	Back-strip. 11	Back-strip. 12	Back-strip. 13	Back-strip. 14	Back-strip. 15	Back-strip. 16	Back-strip. 17
Río Pliego and El Niño Fms	18.- Mioc 1C	100	115	115																
	17.- Mioc 1B	200	223	207	223															
	16.- Mioc 1A	150	175	155	157	175														
El Bosque Fm	15.- Oligoc 2	200	263	210	215	224	263													
	14.- Oligoc 1	750	912	767	774	788	800	912												
Perona Unit	13.- Perona U.	300	308	300	300	300	300	300	308											
Espuña, Valdelaparra, Malvariche, Cánovas and As Fms	12.- Eocene 3	100	230	105	107	111	115	121	146	230										
	11.- Eocene 2	50	129	53	54	57	59	63	80	89	129									
	10.- Eocene 1	125	172	128	129	132	134	137	149	155	158	172								
Cretaceous	9.- Cretac	25	43	26	26	27	28	29	33	35	36	37	43							
Castillón Fm	8.- Jurassic 3	75	91	76	76	77	78	79	83	85	86	87	88	91						
	7.- Jurassic 2	125	155	127	128	129	130	132	139	142	144	145	146	147	155					
	6.- Jurassic 1	125	163	127	128	129	130	132	139	142	144	145	146	147	148	163				
Saladilla Fm	5.- Triassic 4	25	65	26	27	28	29	31	38	42	44	45	47	47	48	50	65			
	4.- Triassic 3	375	471	381	383	388	392	398	419	429	435	438	442	444	446	450	454	471		
	3.- Triassic 2	100	225	103	104	106	108	111	121	126	129	131	133	135	136	138	140	141	225	
	2.- Triassic 1	200	351	206	208	213	217	223	246	258	264	268	273	276	279	284	289	291	308	351
Total thickness		3025	4091	Total thickness reduction = 1066 m																

Table 5

Stratigraphic Unit	Age (My)	Final thickness	Accumulated final thickness	Initial thickness (ESM)	Accumulated initial thickness (ESM)	Initial thickness (SWM)	Accumulated initial thickness (SWM)	Initial thickness (OM)	Accumulated initial thickness (OM)	Initial thickness (PCM)	Accumulated initial thickness (PCM)	Initial thickness (LSM)	Accumulated initial thickness (LSM)	Mean value	Accumulated mean value	Standard deviation from thickness (m)	
Saladilla Fm (700 m)	Triassic-1	240	200	200	279,8	279,8	256,8	256,8	224,6	224,6	261,0	261,0	356,0	356,0	275,6	275,6	4,1
	Triassic-2	230	100	300	137,6	417,4	150,9	407,7	112,0	336,6	207,0	468,0	228,0	584,0	167,1	442,7	4,1
	Triassic-3	217	375	675	458,1	875,5	537,2	944,9	456,1	792,7	485,0	953,0	475,0	1059,0	482,3	925,0	3,1
	Triassic-4	204	25	700	47,7	923,2	37,1	982,0	27,0	819,7	51,0	1004,0	66,0	1125,0	45,8	970,8	1,1
Castillón Fm (350 m)	Jurassic-1	195	125	825	149,9	1073,1	182,4	1164,4	133,9	953,6	158,0	1162,0	164,0	1289,0	157,6	1128,4	1,1
	Jurassic-2	168	125	950	148,5	1221,6	179,1	1343,5	133,2	1086,8	158,0	1320,0	156,0	1445,0	155,0	1283,4	1,1
	Jurassic-3	150	75	1025	88,0	1309,6	107,4	1450,9	78,3	1165,1	94,0	1414,0	92,0	1537,0	91,9	1375,3	1,1
Cretaceous (25 m)	Cretaceous	105	25	1050	36,9	1346,5	33,4	1484,3	26,0	1191,1	49,0	1463,0	43,0	1580,0	37,7	1413,0	8,1
España, Valdelaparra, Malvariche, Cánovas and As Fms (275 m)	Eocene-1	65	125	1175	150,9	1497,4	166,7	1651,0	133,1	1324,2	148,0	1611,0	173,0	1753,0	154,3	1567,3	1,1
	Eocene-2	50	50	1225	88,7	1586,1	73,2	1724,2	55,0	1379,2	98,0	1709,0	131,0	1884,0	89,2	1656,5	2,1
	Eocene-3	40	100	1325	176,6	1762,7	140,0	1864,2	117,1	1496,3	193,0	1902,0	232,0	2116,0	171,7	1828,2	4,1
Perona Thrusting Unit	Perona Unit	35	300	1625	324,1	2086,8	300,0	2164,2	322,3	1818,6	353,0	2255,0	309,0	2425,0	321,7	2149,9	2,1
El Bosque Fm (950 m)	Oligocene-1	30	750	2375	827,5	2914,3	981,1	3145,3	1259,3	3077,9	872,0	3127,0	915,0	3340,0	971,0	3120,9	17,1
	Oligocene.2	25	200	2575	235,5	3149,8	280,0	3425,3	240,5	3318,4	333,0	3460,0	264,0	3604,0	270,6	3391,5	3,1
Río Pliego and El Niño Fms (450 m)	Miocene-1A	23	150	2725	162,1	3311,9	209,0	3634,3	167,5	3485,9	243,0	3703,0	175,0	3779,0	191,3	3582,8	3,1
	Miocene-1B	20	200	2925	208,8	3520,7	246,2	3880,5	218,0	3703,9	208,0	3911,0	223,0	4002,0	220,8	3803,6	1,1
	Miocene-1C	16	100	3025,0	110,5	3631,2	139,3	4019,8	107,5	3811,4	101,0	4012,0	115,0	4117,0	114,7	3918,3	1,1

ESM = Elastic Steinbrenner Method

PCM = Porosity Change Method (Bond et al., 1983)

SWM = Specific Weight Method

LSM = Loadcap Software Method

OM = Oedometric Method

Standard deviation of the initial thicknesses
Variation coefficient of the maximum accumulated values

Table 6

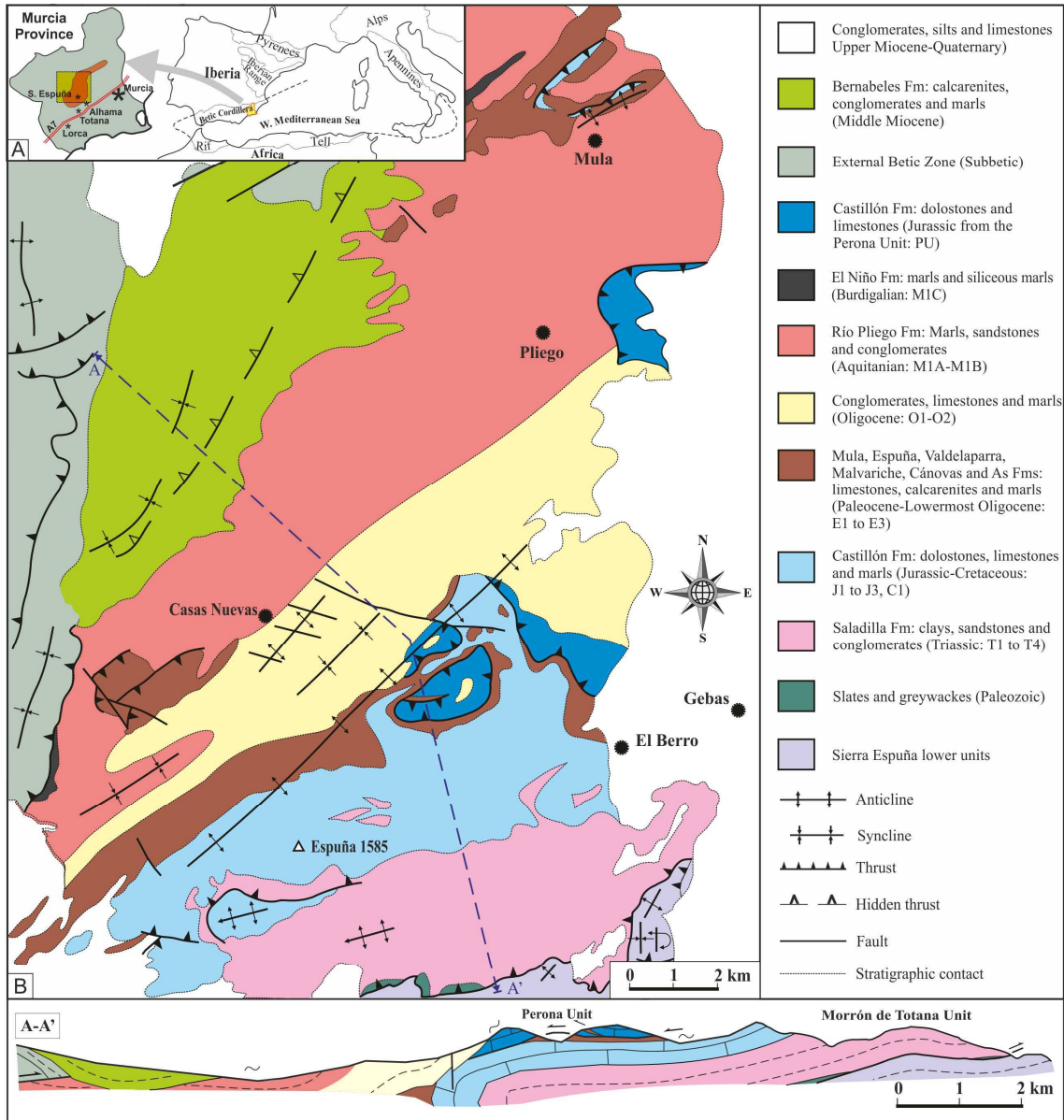


Figure 1

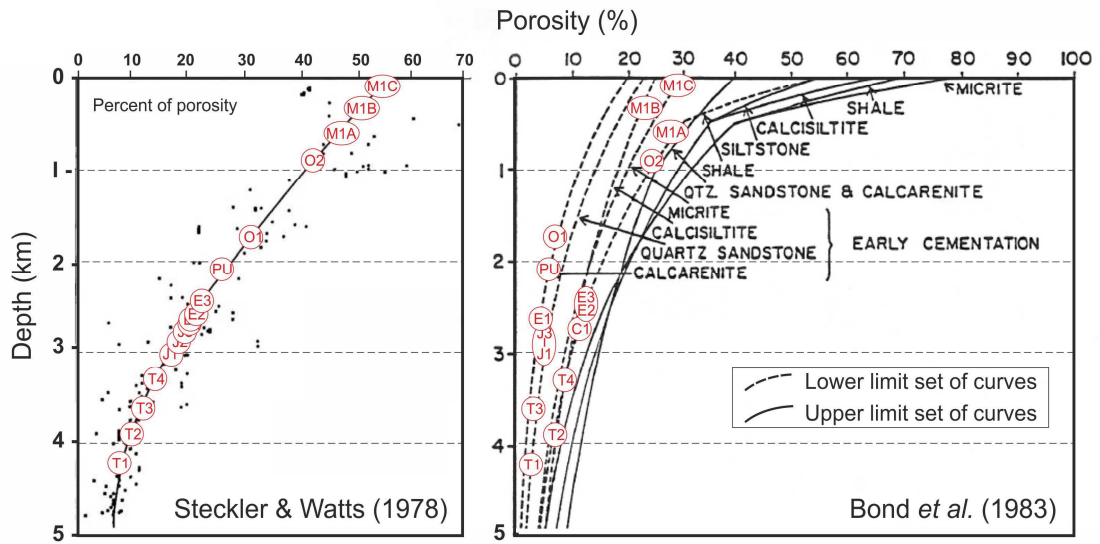


Figure 2

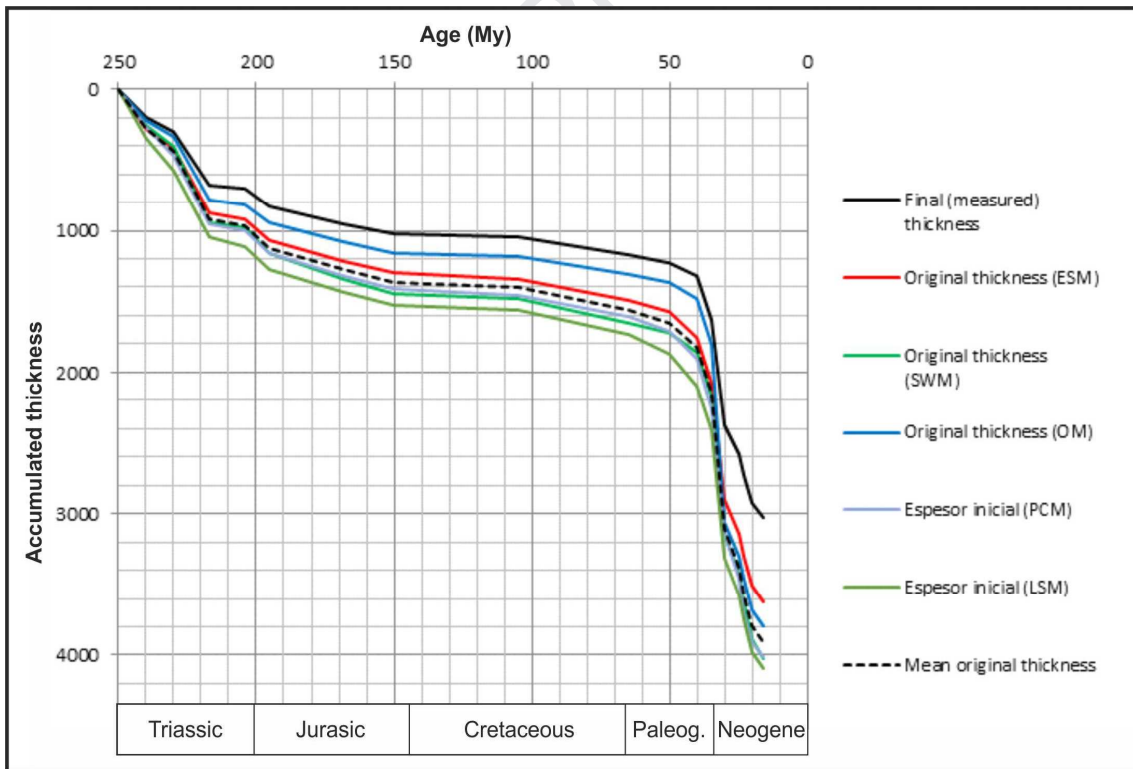


Figure 3

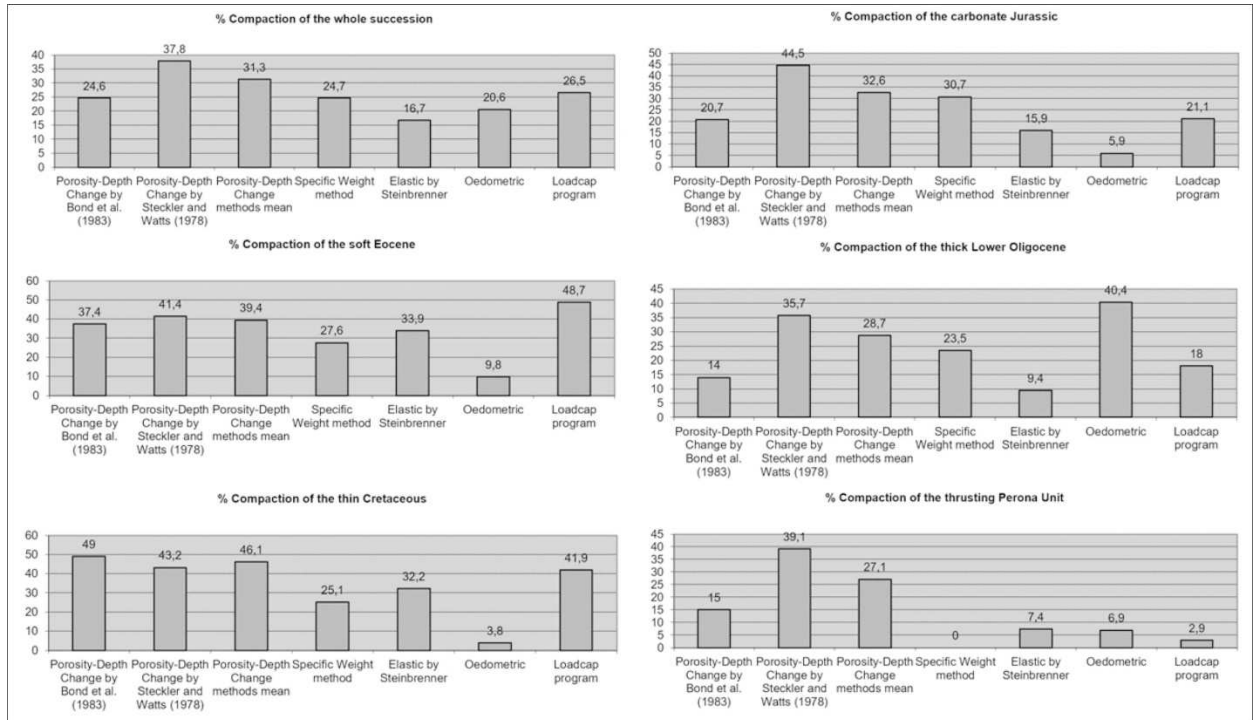


Figure 4

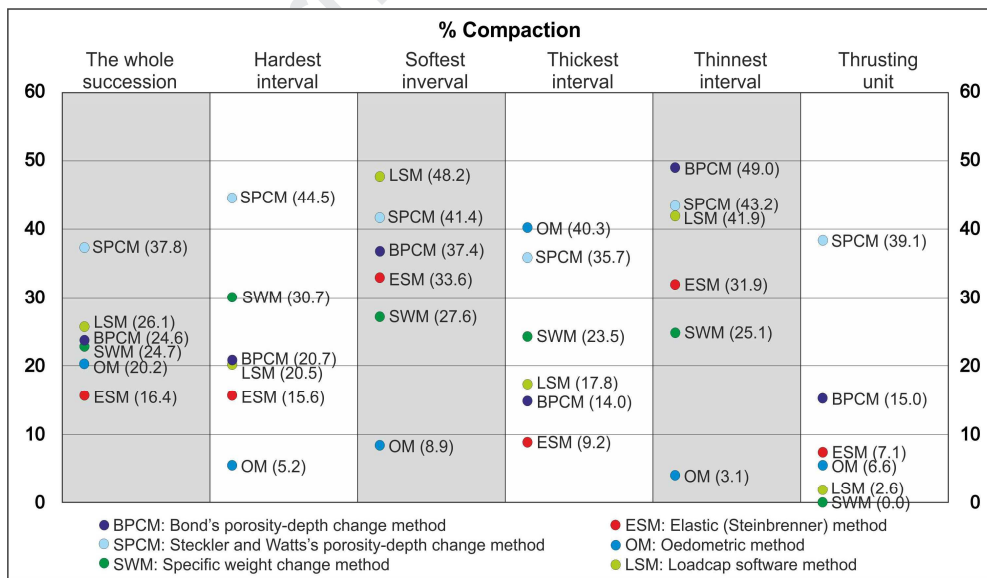


Figure 5

Alternative methods are introduced to calculate compaction.

Inputs for calculations are standards and also coming from engineering studies

Compactions resulting are comparable with porosity-depth lower-limit curves

Mineralogical constraints suggest more accurate specific weight and Loadcap program

Steimbrenner and oedometric show problems with hard rocks and thick beds

Journal Pre-proof